

Novel Methods for Parameter Based Analysis of Myocardial Tissue in MR-Images

A. Hennemuth¹, S. Behrens¹, C. Kuehnel¹, S. Oeltze², O. Konrad¹, H.-O. Peitgen¹

¹MeVis Research GmbH, Universitaetsallee 29, 28359 Bremen, Germany

²Department of Simulation and Graphics, Faculty of Computer Science, University of Magdeburg, Universitaetsplatz 2, 39106 Magdeburg, Germany

ABSTRACT

The analysis of myocardial tissue with contrast-enhanced MR yields multiple parameters, which can be used to classify the examined tissue. Perfusion images are often distorted by motion, while late enhancement images are acquired with a different size and resolution. Therefore, it is common to reduce the analysis to a visual inspection, or to the examination of parameters related to the 17-segment-model proposed by the American Heart Association (AHA). As this simplification comes along with a considerable loss of information, our purpose is to provide methods for a more accurate analysis regarding topological and functional tissue features. In order to achieve this, we implemented registration methods for the motion correction of the perfusion sequence and the matching of the late enhancement information onto the perfusion image and vice versa. For the motion corrected perfusion sequence, vector images containing the voxel enhancement curves' semi-quantitative parameters are derived. The resulting vector images are combined with the late enhancement information and form the basis for the tissue examination. For the exploration of data we propose different modes: the inspection of the enhancement curves and parameter distribution in areas automatically segmented using the late enhancement information, the inspection of regions segmented in parameter space by user defined threshold intervals and the topological comparison of regions segmented with different settings. Results showed a more accurate detection of distorted regions in comparison to the AHA-model-based evaluation.

Keywords: myocardial perfusion, tissue classification, late enhancement

INTRODUCTION

Coronary heart disease causes an ischemia of the supplied myocardium or in worst case a myocardial infarction which is the cause of death for more than seven million people each year [1]. To allow for a preventive therapy, an accurate diagnosis is essential. Cardiac MR provides non-invasive methods for the inspection of myocardial perfusion as well as the detection of infarcted tissue. Thus, it allows for the distinction if tissue is healthy and has sufficient blood supply, if tissue is hypoperfused but could benefit from a therapy or if tissue is already scarred.

Images are usually acquired in short axis slices after the bolus injection of a gadolinium-based contrast agent. The perfusion analysis sequence shows the first pass of the contrast agent and has a high temporal resolution of about 1 second depending on the patient's ECG. Hence, even with parallel imaging technique, no high spatial resolution is possible with current scanner technology and normally only 3 to 6 image slices with a thickness of 6 to 10 mm and gap about 6 mm are acquired.

Fig. 1 shows an example dataset with four perfusion slices (yellow border). The curves on the right image illustrate the intensity change over time due to the wash-in and wash-out of the contrast agent, which is related to the perfusion. The myocardial perfusion is measured via so called semi-quantitative parameters describing the behaviour of the intensity curves derived from the image sequence.

As acute or chronically infarcted tissue shows an enhanced distribution volume for Gd-DTPA, it can be imaged 10 to 30 minutes after bolus injection as bright image regions. For this purpose, short axis slices with about 8 mm thickness with or without spacing are acquired (slices with orange border in Fig. 1).

The analysis of the perfusion sequences requires a pre-processing step to compensate motion artefacts from breathing, myocardium contraction and patient motion. Due to the contrast changes between the images in the perfusion sequence this is a difficult problem and there exist various approaches using different image features [2-6] and model-based

assumptions regarding shape [6-8] or intensity courses [8-10]. As methods available in commercial software tools commonly offer only rough motion correction, the parameter analysis is often performed for intensity curves of manually defined myocardial segments according to the AHA-17-segment-model [11].

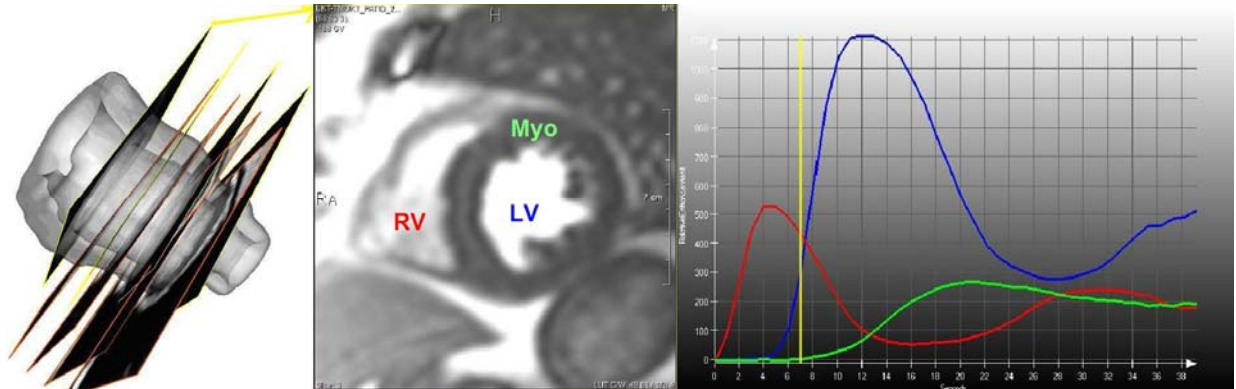


Fig. 1: Example data from the test set :

Left image: Left ventricle together with slices from the late enhancement image (red) and the perfusion sequence (yellow). The figure illustrates the differences in slice spacing/thickness and orientation.

Middle image: Short axis perfusion image with contrast agent in right ventricle (RV) and left ventricle (LV) but not yet in myocardium (Myo)

Right image: Time-intensity curves of right ventricle (red), left ventricle (blue) and myocardium (green)

The detection of scarred tissue in late enhancement images requires a definition of a suitable threshold to distinguish between healthy tissue and infarction. The clinically accepted method uses the histogram of a user defined healthy myocardial region to determine a threshold at position $\mu + 2\sigma$ [12;13]. Though the infarction's transmural extent is of high interest, standard analysis methods only yield the portion of voxels above the threshold per myocardial segment. The problem of image misalignment in MR examination due to patient and breathing motion has been addressed in previous publications in the context of model-based analysis [14] according the AHA-model. For the alignment of MR image slices acquired at different time points Lötjönen et al. propose a 3D approach extending slice thickness to close gaps between them [15], while Barajas et al. determine intersections of slices without thickness and only consider these for registration [16]. Both methods focus on the alignment of slices for functional analysis and thus only compensate translational motion.

Though approaches for supporting combined analysis of delayed enhancement and myocardial function [9], and the relation of morphologic with perfusion measurements [17] already exist, the combination of information from perfusion analysis and late enhancement segmentation is currently only supported segment-based [4]. This can produce misleading results, as late enhancement images and perfusion images can differ in orientation and image region (Fig. 1). For these segments, boolean parameters are used to come to a rough tissue classification [18].

The purpose of our work is to provide methods for a differentiated tissue analysis regarding location, shape, and perfusion characteristics through the combined analysis of perfusion and late enhancement parameters in the original images' resolution.

METHODS

1. Computation of parameter images

To extract myocardial perfusion parameters, a motion correction of the image region of interest is performed first. For this purpose, an affine registration (1) followed by a cubic B-Spline registration (2) step is applied:

$$\begin{pmatrix} x_{t1} \\ y_{t1} \end{pmatrix} = \underbrace{\begin{pmatrix} \cos(\alpha) & \sin(\alpha) \\ -\sin(\alpha) & \cos(\alpha) \end{pmatrix}}_{\text{Rotation}} \underbrace{\begin{pmatrix} 1 & 0 \\ s_2 & 1 \end{pmatrix}}_{\text{Shearing}} \underbrace{\begin{pmatrix} s_x & 0 \\ 0 & s_y \end{pmatrix}}_{\text{Scaling}} \begin{pmatrix} x \\ y \end{pmatrix} + \underbrace{\begin{pmatrix} t_x \\ t_y \end{pmatrix}}_{\text{Translation}} \quad (1)$$

$$\begin{pmatrix} x_{t2} \\ y_{t2} \end{pmatrix} = \sum_j \sum_i \begin{pmatrix} \alpha_{ij} \\ \beta_{ij} \end{pmatrix} \cdot \underset{\text{CubicB-Spline-Functions}}{B_i(x_{t1}) \cdot B_j(y_{t1})} \quad (2)$$

The similarity is measured with *normalized mutual information*, according to formula (3) and (4):

$$h \left(\underset{\text{Reference Image}}{R} \right) = - \sum_{g \in R} p_R(g) \cdot \ln p_R(g) \quad (3)$$

$$h \left(\underset{\text{Floating Image}}{F} \right) = - \sum_{g \in F} p_F(g) \cdot \ln p_F(g)$$

$$h(R, F) = - \sum_{g_1 \in R} \sum_{g_2 \in F} p_{R,F}(g_1, g_2) \ln p_{R,F}(g_2, g_1)$$

Entropy

$$NMI = \frac{h(R) + h(F)}{h(R, F)} \quad (4)$$

Optimization is achieved by application of the so called *Simplex* algorithm by Nelder and Mead [19].

To minimize interpolation artefacts, every image of the sequence is matched on its corrected predecessor, to which we assume the least difference by contrast change. From the motion corrected sequences, vector images of semi-quantitative enhancement parameters such as time-to-peak, upslope, area-under-curve and peak-enhancement are derived. Therefore regularization over time is applied to achieve more robustness without loss of spatial resolution.

To register the late enhancement data with these images, a first rough matching uses the DICOM coordinate information. For each slice of the perfusion sequence the corresponding region in the late enhancement image is reformatted to match orientation and resolution and cropped for the subsequent registration (Fig. 2). In the perfusion sequence, we choose the image of the last baseline time point, because it shows the most similar contrast distribution with the late enhancement image having high intensity values in right and left ventricle and low ones in myocardial tissue (Fig. 1).

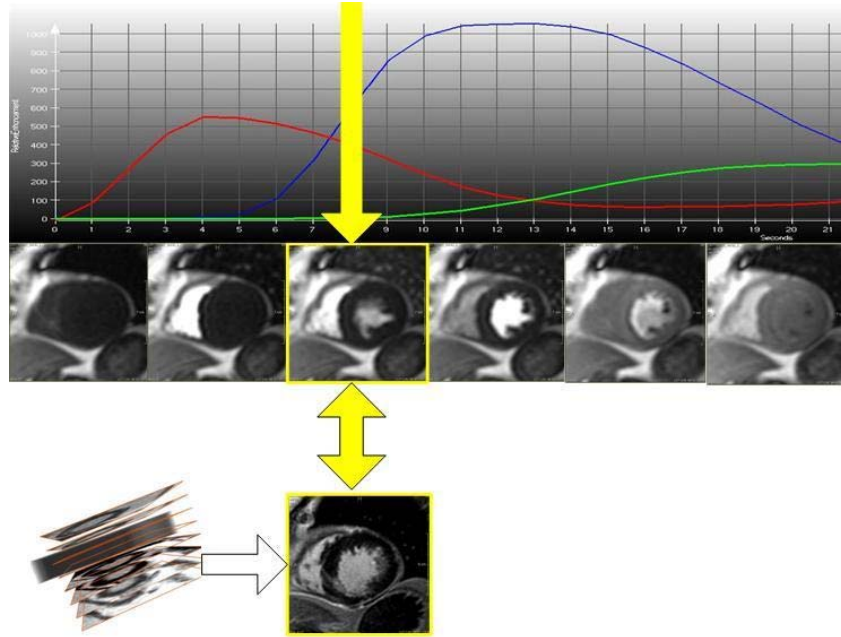


Fig. 2: Registration of perfusion and late enhancement images: The curve in the upper image shows the enhancement curves corresponding to the right ventricle (red), the left ventricle (blue) and the myocardium (green). The yellow arrow shows time point and corresponding image selected for registration. The lower image shows the portion of the late enhancement image to be matched.

The subsequent registration is performed for both directions and like in the motion correction step searches for an optimal affine transformation followed by an elastic one (Formula (1) and (2)). Similarity is measured with normalized mutual information (Formula (3) and (4)) and parameters are optimized using the simplex algorithm. Transformation parameters are stored with the case information and can be used for different combination purposes. On the one hand, perfusion related image data can be transformed for visualization with results from late enhancement derived 3D results. On the other hand, transformed data and results from the late enhancement image can be added to the vector images derived from the perfusion sequence to allow for a joint visualization and analysis.

2. Segmentation and Visualization

For the analysis of data we propose different modes of combination:

2.1. Late Enhancement and Perfusion

First, a method was developed for the automatic detection of regions showing delayed enhancement and inspection of the perfusion parameter distributions in these regions. The algorithm automatically derives a threshold interval from the myocardium's histogram using a Gaussian mixture model. To avoid the segmentation of noise or distortions at the edges of the myocardium segmentation, seed points are detected in the inner part of the myocardial wall and used for a subsequent region growing with the previously determined threshold.

For the corresponding region in the perfusion sequence, the enhancement curve as well as the parameter distributions are derived and inspected. Furthermore, the transformation describing the registration of the perfusion image with the late enhancement image can be used to transform the parameter image for visualization with the surfaces of the ventricle and late enhancement segmentation. Fig. 3 depicts the visualization modes for comparison.

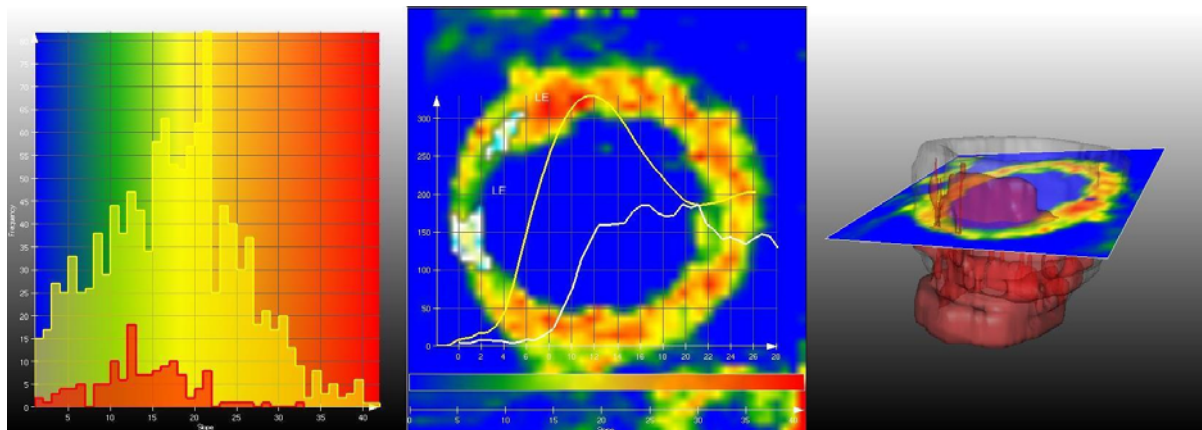


Fig. 3: Comparison of late enhancement segmentation with myocardial perfusion

Left image: The parameter distribution of the whole myocardium (yellow) and the segmented late enhancement region (red).

Middle image: Parameter image showing the upslope of the enhancement curves, the white overlay shows the segmented late enhancement region. The white curve shows the enhancement curve corresponding to the overlay region while the yellow curve represents the enhancement curve of the segmented myocardium.

Right image: 3D surface representation of the segmentation results from the late enhancement image combined with a texture representation of the transformed parameter image slice.

2.2. Parameter-based Segmentation

In the parameter vector image, segmentations can be performed for single parameters or parameter combinations.

The user defines segmentation intervals in the histograms of the different myocardial parameter distributions. The parameters to consider can be selected. There are three modes for the inspection of the defined intervals. First, the components of the parameter image vectors can be treated separately to allow for a comparison of the segmentation results. The selected parameters can also be regarded in combination. In doing so, either the voxel sets meeting all interval conditions, or those with at least one component inside the defined parameter limits can be determined. Resulting regions are shown in 2D as an overlay to the perfusion image as well as in an idealized 3D surface rendering (Fig. 1).

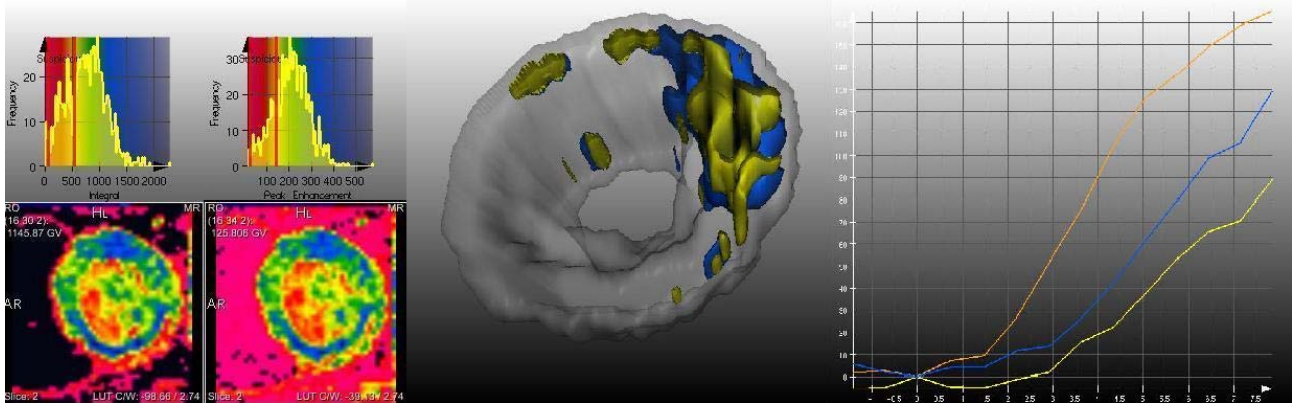


Fig. 4: Segmentation in parameter images

Left image: Parameter images and histograms for peak enhancement and area under curve. The red splitters show the parameter range selected for segmentation.

Middle image: Separately segmented region for the defined parameter intervals (blue: area under curve, yellow: peak enhancement)

Right image: Corresponding enhancement curves for myocardium, blue and yellow region

To get an impression of the segmentation's transmural extent, the distance from the myocardial surface is computed [20] and shown in the 3D visualization.

To further examine the regions defined by specific parameter ranges, averaged enhancement curves for segmented regions can be inspected.

RESULTS

The described algorithms were integrated into the prototypical application *MeVisCardioPerfusion*, which was developed within the VICORA research project. By means of this application, methods could be applied to a test set of 18 clinical examinations of patients suffering from coronary heart disease. All image datasets contained perfusion sequences under rest and pharmacologically induced stress as well as 16 late enhancement images. The images were acquired using three different scanners (Siemens Sonata, Siemens Avanto and Siemens Trio) with a TurboFlash 2D sequence and a contrast agent injection of 0,075 mmol to 0.1 mmol Gd-DTPA (Schering, Berlin). Perfusion sequences consisted of 3 to 4 short-axis-slices with 6 mm to 10 mm thickness and a slice spacing between 14 and 20 mm. The resolution in plane was 1.25 x 1.25mm to 1.875 x 1.875 mm. 20 to 40 time points were measured over a period of 17 to 38 seconds. For late enhancement imaging 4 to 11 slices were acquired with a thickness of 6 to 10 mm and a spacing of 10 mm. Here the resolution in plane was between 1.25 x 1.25 mm and 1.484 x 1.484 mm.

For all patients the findings of the clinical MR examination and a conventional catheter angiography were available. The MR examination findings state, which of the three main coronary branches (RCA, LAD, LCX) are believed to cause a hypoperfusion, while the catheter angiographic findings contain information about the degree of stenosis in segments of the coronary artery tree.

To determine if plausible results can be achieved with the proposed methods, the datasets were inspected using the prototypical application. Segmentations were done applying threshold intervals indicating low or no enhancement [21]. For slope, peak-enhancement, area-under-curve thresholds below the most frequent value were chosen, while for time-to-peak a higher threshold was selected. To enable a comparison with the AHA-segment-model-based clinical findings, the portion of segmented AHA-segment was determined for the segmentation results.

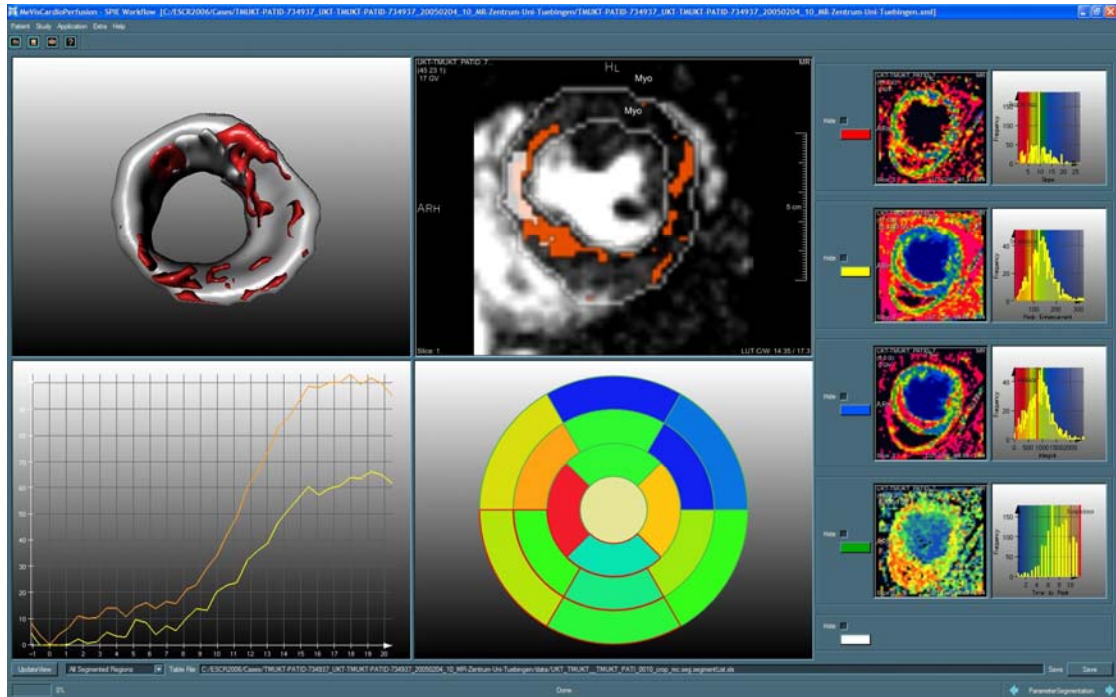


Fig. 5: Determination of suspicious regions and their portion per AHA-model-segment. The four small images in the right panel show the distribution of the four considered perfusion parameters and the selected segmentation intervals. The upper two viewers show the myocardium and the segmented region as surfaces in 3D and as overlay to the source image. While the lower left viewer shows the perfusion curve corresponding to the segmented region (yellow) in comparison with the myocardial perfusion curve (orange), the lower right viewer shows the portion of segmented area per AHA-segment in the so called Bulls-Eye-Plot.

In the subsequent evaluation, first we determined if the affected segments belonged to the supply region of a coronary segment with known stenosis. Second, we checked, if the detected regions' locations matched the information from the clinical MR examination, and third determined if additional information corresponding with the catheter examination was computed.

One dataset could not be analyzed due to strong motion perpendicular to the image plane, which can not be compensated by the applied correction method. In two other datasets due to image artefacts only parts of the myocardium could be examined. In all other datasets motion correction and parameter computation could be performed successfully.

Late enhancement was detected in 10 datasets. For 30 out of 41 affected segments corresponding stenoses of a degree between 75% and 100% were indicated in the supplying coronary branches. Eleven segments did not directly belong to arteries with known stenosis according to the AHA-model, but were adjacent to segments which could be assigned.

Regions with a believed hypoperfusion were detected in all datasets. For evaluation only those segments with a portion of more than 25% segmented region were considered. From 79 concerned segments, 42 could be associated with reported stenosis, while 27 were located adjoining such segments. Regions detected in 10 other segments could neither be correlated with the angiographic nor with the MR based findings. In all but one dataset the finding from the MR examination was agreed. In 7 datasets additional distorted regions were detected, which corresponded with stenosed coronary branches.

To determine, whether voxel-based analysis allows for the detection of hypoperfused areas, which would not be conspicuous with segment-based analysis, the parameter values of the affected segments were inspected. If the parameter values of the segment's average curve were outside the parameter intervals chosen for segmentation, the segment was considered as disregarded. From 79 segments affected by regions detected in the parameter images, 43 showed conspicuous enhancement curves. 11 segments with low perfusion curves were located adjacent to affected segments.

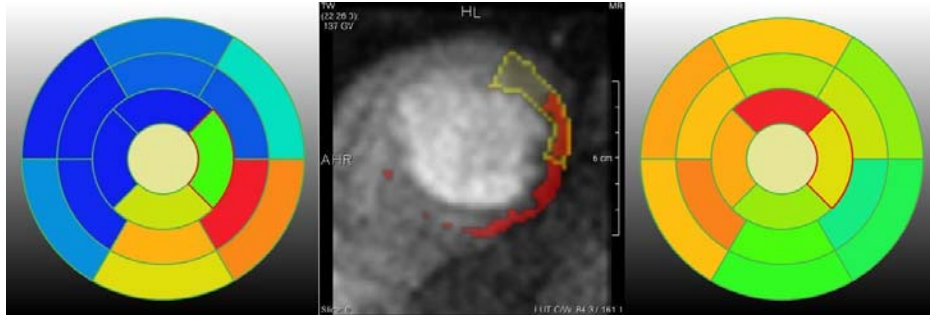


Fig. 6: Segmentation result in relation to the AHA-segment-model:

Left image: Bulls-eye-plot showing the portion of segmented region per AHA-segment.

Middle image: Overlay of segmentation result in the source image (red). The yellow border shows the myocardial region corresponding to segment 14 which is framed red in the bulls-eye-plots.

Right image: Bulls-eye-plot showing the peak-enhancement-parameter value derived from the segment's enhancement curve.

For 11 image datasets with late enhancement segmentation, which correlated well with the clinical findings, the combined view of late enhancement segmentation and perfusion parameters, was rated on the basis of a visual inspection. There were three grading categories:

1. Possibly misleading information due to unsuccessful registration
2. Plausible results
3. Helpful information through combination

Fig. 7 shows examples for these categories.

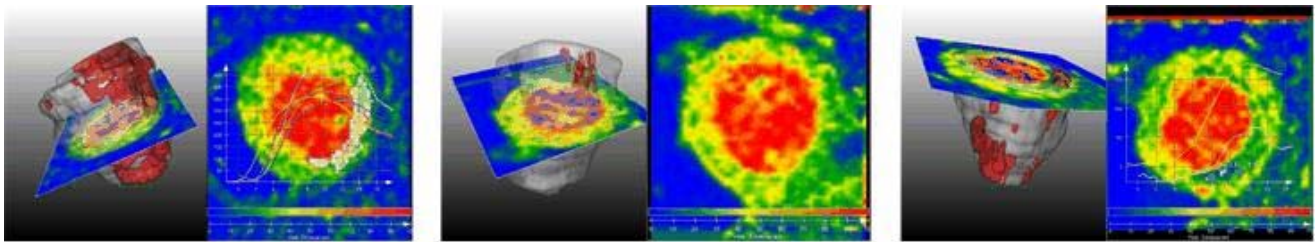


Fig. 7: Examples for rating categories

Left image: category 1: After registration the segmented late enhancement region is partly located in the bloodpool and thus the corresponding enhancement curve is high

Middle image: category 2: As the detected late enhancement lies outside of the perfusion image, no comparison is possible. This information might at least be helpful to understand the mismatch between segment-based results derived from perfusion and late enhancement images.

Right image: category 3: The detected late enhancement matches the image region in the lower part of the image showing very low perfusion values. Parameter values in the surrounding indicate a distorted but active perfusion.

From 11 inspected datasets three were categorized 1 while four belonged to category 2 and five to category 3. In two datasets classified as category 2 the image region affected with late enhancement was not acquired for perfusion analysis. Thus, no helpful comparison was possible.

DISCUSSION

For all but three datasets at least partial results could be derived from the given image data. As only three image slices with a gap of around 6 mm were acquired, no correction of out-of-plane-motion is suggestive.

For the registration of perfusion and late enhancement images, we used an approach related to that of Barajas et al [16], because due to the huge gap between the image slices a padding to a 3D volume like proposed in [15] would produce implausible information. As in contrast to the problem of aligning short and long axis slices, the difference in orientation is low, the thickness of the perfusion slices is used to detect the late enhancement image region to be

reformatted and used for registration and affine and elastic transformations were allowed to compensate motion due to different heart phases as well. Though misaligned late enhancement slices (Fig. 8) and contrast differences in late enhancement regions, most likely also occur, when registering with functional images, this problem is not reported for other approaches using mutual information. Here, the model- and landmark-based approach of Swingen et al might be advantageous [22].

The use of parameter maps for the analysis of myocardial perfusion has been shown to be useful in clinical application [23]. Though most detected regions detected in the parameter images agreed well with the segments dependent on stenosed arteries, there were some mismatches. This could on the one hand be down to the definition of the myocardial segments, which is based on the given image information and does not consider the slice location relative to the ventricle. On the other hand, the anatomy of the coronary tree is known to show strong variation in origin and course of coronary branches [24]. Thus application of the standard model may lead to false assumptions regarding dependencies.

Comparison with segment-based analysis shows a higher sensitivity in the detection of compact distortions, especially if these are located on the border of two neighbouring segments. The threshold based segmentation performed in these images, showed different patterns of shape and location. For the analysis of function and late enhancement, the distortions' transmuralities is known to be of high interest. Using the segmentation information such results could be derived on hypoperfused regions as well.

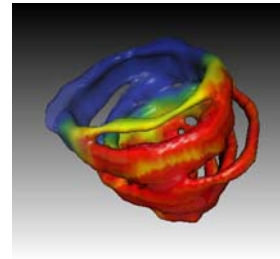


Fig. 8: Surface reconstruction of left ventricle from late enhancement image data with misaligned slices

CONCLUSIONS

We developed a software tool dedicated to the combined analysis of myocardial perfusion and late enhancement analysis. The implemented methods were applied to a test set of 18 clinical datasets and results were compared to clinical findings from catheter angiography and MR examination. The results showed a good correspondence between findings from catheter angiography and regions considered as scarred or hypoperfused according to the performed segmentation. Compared with the MR-based findings the delivered information was extended. Compared to the standardized region based perfusion analysis, the methods showed a higher sensitivity and provide additional information on the shape of detected distortions. This indicates that clinically useful information can be delivered by these methods, which extends the standard evaluation available in clinical routine.

For the combination of perfusion parameter results and late enhancement detection, some restrictions were found. The occurrence of misalignments between the slices of late enhancement images indicates that a correction step should be introduced before registration with the perfusion images. Furthermore, the problem of misregistration in datasets with large endocardial late enhancement regions has to be addressed, either by choosing another similarity measure or pre-masking the affected image regions. The visualization of spatial correspondences, corresponding parameter distributions and curves of regions segmented in late enhancement and parameter images with suitable registration delivered helpful information regarding the area surrounding infarctions. Further work on the reliable computation of the matching transformation is therefore desirable.

Altogether, the provided have shown to be a good basis for further investigations on clinically applicable methods for the detection and visualization of infarctions and perfusion defects. Future work should focus on the development of automatic classification methods, the consideration of perfusion reserve indices for the comparison of rest and stress perfusion and better visualizations of parameter combinations.

ACKNOWLEDGEMENTS

We would like to thank Dr. A. Seeger, Dr. S. Miller and Dr. M. Fenchel for the fruitful cooperation within the VICORA research project funded by the German Federal Ministry for Education and Research.

REFERENCES

- [1] Mackay J, Mensah GA. *The Atlas of Heart Disease and Stroke*. http://www.who.int/cardiovascular_diseases/en/. 2004.

- [2] Bidaut LM, Vallee JP. *Automated registration of dynamic MR images for the quantification of myocardial perfusion*. J Magn Reson Imaging 2001; 13(4):648-655.
- [3] Bracoud L, Vincent F, Pachai C, Canet E, Croisille P, Revel D *Automatic Registration of MR First-Pass Myocardial Perfusion Images*. Lecture Notes in Computer Science: Springer-Verlag GmbH, 2003, pp. 215-223.
- [4] Breeuwer M, Paetsch I, Nagel E, Muthupillai R, Flamm S, Plein S et al. *The detection of normal, ischemic and infarcted myocardial tissue using MRI*. International Congress Series 1256, 1153-1158. 2003. CARS 2003.
- [5] Gupta SN, Solaiyappan M, Beache GM, Arai AE, Foo TK. *Fast method for correcting image misregistration due to organ motion in time-series MRI data*. Magn Reson Med 2003; 49(3):506-514.
- [6] Sun Y, Jolly M-P, Moura JMF *Contrast-Invariant Registration of Cardiac and Renal MR Perfusion Images*. 2004; 10.1007/b100265: Springer Berlin / Heidelberg, 2004, pp. 903-910.
- [7] Bansal R, Funka-Lea G *Integrated Image Registration for Cardiac MR Perfusion Data*. Lecture Notes in Computer Science: Springer-Verlag, 2002, pp. 659-666.
- [8] Stegmann MB, Olafsdottir H, Larsson HB. *Unsupervised motion-compensation of multi-slice cardiac perfusion MRI*. Med Image Anal 2005; 9:394-410.
- [9] Discher A, Rougon N, Preteux F *An unsupervised approach for measuring myocardial perfusion in MR image sequences*. 2005
- [10] Rougon N, Discher A, Preteux F *Region-driven statistical non-rigid registration: application to model-based segmentation and tracking of the heart in perfusion MRI*. San Diego, CA: 2005, pp. 148-159.
- [11] Cerqueira MD, Weissman NJ, Dilsizian V, Jacobs AK, Kaul S, Laskey WK et al. *Standardized myocardial segmentation and nomenclature for tomographic imaging of the heart: a statement for healthcare professionals from the Cardiac Imaging Committee of the Council on Clinical Cardiology of the American Heart Association*. Circulation 2002; 105(4):539-542.
- [12] Kim RJ, Hillenbrand HB. *Evaluation of myocardial viability by MRI*. Herz 2000; 25 %6(4):417-430.
- [13] Kolipaka A, Chatzimavroudis GP, White RD, O'donnell TP, Setser RM. *Segmentation of non-viable myocardium in delayed enhancement magnetic resonance images*. The International Journal of Cardiovascular Imaging (formerly Cardiac Imaging) 2005; 21(2):303-311.
- [14] McLeish K, Hill DLG, Atkinson D, Blackall JM, Razavi R. *A Study of the Motion and Deformation of the Heart Due to Respiration*. IEEE Trans Med Imaging 2002; 21(9).
- [15] Lotjonen J, Pollari M, Kivisto S, Lauerma K. *Correction of movement artifacts from 4-D cardiac short-and long-axis MR data*. MICCAI (2) 2004;405-412.
- [16] Barajas J, Caballero KL, Barnes JG, Carreras F, Pujadas S, Radeva P *Correction of Misalignment Artifacts Among 2-D Cardiac MR Images in 3-D Space*. Springer Berlin / Heidelberg, 2006
- [17] Sturm B, Powell KA, Stillman AE, White RD. *Registration of 3D CT angiography and cardiac MR images in coronary artery disease patients*. Int J Cardiovasc Imaging 2003; 19(4):281-293.
- [18] Oeltze S, Grothues F, Hennemuth A, Kuß A, Preim B *Integrated Visualization of Morphologic and Perfusion Data for the Analysis of Coronary Artery Disease*. 2006; 2006
- [19] Press WH, Flannery BP, Teukolsky SA, Vetterling WT. *Numerical Recipes in C - The Art of Scientific Computing*. Cambridge: Cambridge University Press, 1988.
- [20] Borgefors G. *Distance transformations in digital images*. Computer Vision, Graphics, and Image Processing 1986; 34(3):344-371.
- [21] Bremerich J, Buser P, Bongartz G. *Diagnostik der koronaren Herzkrankheit mit CT und MRT*. Radiologie up2Date 2005;(1):13-24.
- [22] Swingen C, Seethamraju RT, Jerosch-Herold M. *An approach to the three-dimensional display of left ventricular function and viability using MRI*. Int J Cardiovasc Imaging 2003; 19(4):325-336.
- [23] Thiele H, Plein S, Breeuwer M, Ridgway J, Higgins D, Thorley PJ et al. *Color-Encoded Semiautomatic Analysis of Multi-Slice First-Pass Magnetic Resonance Perfusion: Comparison to Tetrofosmin Single Photon Emission Computed Tomography Perfusion and X-Ray Angiography*. The International Journal of Cardiovascular Imaging (formerly Cardiac Imaging) 2004; V20(5):371-384.
- [24] Duran C, Kantarci M, Durur S, I, Gulbaran M, Sevimli S, Bayram E et al. *Remarkable anatomic anomalies of coronary arteries and their clinical importance: a multidetector computed tomography angiographic study*. J Comput Assist Tomogr 2006; 30(6):939-948.